

(2)

College of Earth and Mineral Sciences

PENNSTATE

AFOSR-TR- 89-0392



AIR FORCE OFFICE OF SCIENTIFIC RESEARCH (AFOSR)
AFOSR-TR-89-0392

Approved on this
date: APR 190-12.

Chief, Technical Information Division

DTIC
ELECTE
APR 17 1989
S D
D 03

Approved for public release;
distribution unlimited.

AD-A207 161

Grant No. AFOSR-85-0298

Final Report

to

Air Force Office of Scientific Research

Bolling, AFB, DC 20332

HIGH TEMPERATURE OXIDATION STUDIES ON ALLOYS CONTAINING
DISPERSED PHASE PARTICLES AND CLARIFICATION OF THE
MECHANISM OF GROWTH OF SiO_2

Submitted to: Dr. Liselotte J. Schioler

Submitted by: R. Yan, B. Munn and Dr. G. Simkovich

DISTRIBUTION STATEMENT A

Approved for public release;
Distribution Unlimited

January

1989

89

4

12

064

PENN STATE

College of Earth and Mineral Sciences

Undergraduate Majors

Ceramic Science and Engineering, Fuel Science, Metals Science and Engineering, Polymer Science; Mineral Economics; Mining Engineering, Petroleum and Natural Gas Engineering; Earth Sciences, Geosciences; Geography; Meteorology.

Graduate Programs and Fields of Research

Ceramic Science and Engineering, Fuel Science, Metals Science and Engineering, Polymer Science; Mineral Economics; Mining Engineering, Mineral Processing, Petroleum and Natural Gas Engineering; Geochemistry and Mineralogy, Geology, Geophysics; Geography; Meteorology.

Universitywide Interdisciplinary Graduate Programs Involving EMS Faculty and Students

Earth Sciences, Ecology, Environmental Pollution Control Engineering, Mineral Engineering Management, Solid State Science.

Associate Degree Programs

Metallurgical Engineering Technology (Shenango Valley Campus).

Interdisciplinary Research Groups Centered in the College

C. Drew Stahl Center for Advanced Oil Recovery, Center for Advanced Materials, Coal Research Section, Earth System Science Center, Mining and Mineral Resources Research Institute, Ore Deposits Research Group.

Analytical and Characterization Laboratories (Mineral Constitution Laboratories)

Services available include: classical chemical analysis of metals and silicate and carbonate rocks; X-ray diffraction and fluorescence; electron microscopy and diffraction; electron microprobe analysis; atomic absorption analysis; spectrochemical analysis; surface analysis by secondary ion mass spectrometry (SIMS); and scanning electron microscopy (SEM).

The Pennsylvania State University, in compliance with federal and state laws, is committed to the policy that all persons shall have equal access to programs, admission, and employment without regard to race, religion, sex, national origin, handicap, age, or status as a disabled or Vietnam-era veteran. Direct all affirmative action inquiries to the Affirmative Action Officer, Suzanne Brooks, 201 Willard Building, University Park, PA 16802; (814) 863-0471.
U. Ed. 87-1027
Produced by the Penn State Department of Publications

A-107161

REPORT DOCUMENTATION PAGE

1a. REPORT SECURITY CLASSIFICATION UNCLASSIFIED		1b. RESTRICTIVE MARKINGS													
2a. SECURITY CLASSIFICATION AUTHORITY		3. DISTRIBUTION/AVAILABILITY OF REPORT APPROVED FOR PUBLIC RELEASE; DISTRIBUTION UNLIMITED													
2b. DECLASSIFICATION/DOWNGRADING SCHEDULE		5. MONITORING ORGANIZATION REPORT NUMBER(S) AFOSR-TR-89-0392													
4. PERFORMING ORGANIZATION REPORT NUMBER(S)		7a. NAME OF MONITORING ORGANIZATION AFOSR/NE													
6a. NAME OF PERFORMING ORGANIZATION Dept. of Met. Sci. & Eng. The Pennsylvania State Univ		7b. ADDRESS (City, State and ZIP Code) BLDG. 410 BOLLING AFB, DC 20332-6448													
6b. OFFICE SYMBOL (If applicable)		9. PROCUREMENT INSTRUMENT IDENTIFICATION NUMBER AFOSR 85-0298													
8a. NAME OF FUNDING/SPONSORING ORGANIZATION AFOSR		10. SOURCE OF FUNDING NOS. <table border="1"><thead><tr><th>PROGRAM ELEMENT NO.</th><th>PROJECT NO.</th><th>TASK NO.</th><th>WORK UNIT NO.</th></tr></thead><tbody><tr><td>AFOSR</td><td>85-0298</td><td></td><td></td></tr><tr><td>61102F</td><td>2306</td><td>A2</td><td></td></tr></tbody></table>		PROGRAM ELEMENT NO.	PROJECT NO.	TASK NO.	WORK UNIT NO.	AFOSR	85-0298			61102F	2306	A2	
PROGRAM ELEMENT NO.	PROJECT NO.	TASK NO.	WORK UNIT NO.												
AFOSR	85-0298														
61102F	2306	A2													
8b. OFFICE SYMBOL (If applicable) NE															
8c. ADDRESS (City, State and ZIP Code) Bolling AFB Washington, D.C. 20332															
11. TITLE (Include Security Classification) High Temperature Oxidation..... ON BACK Growth of SiO₂															
12. PERSONAL AUTHOR(S) G. Simkovich															
13a. TYPE OF REPORT Final Report		13b. TIME COVERED FROM 15 Aug. 85 TO 31 Dec. 88													
		14. DATE OF REPORT (Yr., Mo., Day) 1989, Feb, 14													
15. PAGE COUNT															
16. SUPPLEMENTARY NOTATION															
17. COSATI CODES <table border="1"><thead><tr><th>FIELD</th><th>GROUP</th><th>SUB. GR.</th></tr></thead><tbody><tr><td></td><td></td><td></td></tr><tr><td></td><td></td><td></td></tr><tr><td></td><td></td><td></td></tr></tbody></table>		FIELD	GROUP	SUB. GR.										18. SUBJECT TERMS (Continue on reverse if necessary and identify by block number)	
FIELD	GROUP	SUB. GR.													
19. ABSTRACT (Continue on reverse if necessary and identify by block number) <p>A wide variety of high temperature oxidation tests have been conducted on Fe and Ni based alloys. Especially, the effects of dispersion phase particles on the oxidation properties were well studied.</p>															
20. DISTRIBUTION/AVAILABILITY OF ABSTRACT UNCLASSIFIED/UNLIMITED <input checked="" type="checkbox"/> SAME AS RPT. <input type="checkbox"/> DTIC USERS <input type="checkbox"/>		21. ABSTRACT SECURITY CLASSIFICATION UNCLASSIFIED													
22a. NAME OF RESPONSIBLE INDIVIDUAL SCHROER		22b. TELEPHONE NUMBER (Include Area Code) (202) 767-4933													
		22c. OFFICE SYMBOL NE													

11. STUDIES ON ALLOYS CONTAINING DISPERSED PHASE PARTICLES AND CLARIFICATION OF THE MECHANISM OF GROWTH OF SiO_2

Grant No. AFOSR-85-0298

Final Report

to

**Air Force Office of Scientific Research
Bolling, AFB, DC 20332**

**HIGH TEMPERATURE OXIDATION STUDIES ON ALLOYS CONTAINING
DISPERSED PHASE PARTICLES AND CLARIFICATION OF THE
MECHANISM OF GROWTH OF SiO_2**

Submitted to: Dr. Liselotte J. Schioler

Submitted by: R. Yan, B. Munn and Dr. G. Simkovich

January 1989

Accession For	
NTIS CRA&I	<input checked="checked" type="checkbox"/>
DTIC TAB	<input type="checkbox"/>
Unannounced	<input type="checkbox"/>
Justification	
By _____	
Distribution /	
Availability Codes	
Dist	Avail and/or Special
A-1	

Introduction

↓
In most binary transition metal alloys, additions of Cr are used to promote the formation of a protective Cr_2O_3 layer. Once formed, this layer acts as a barrier between the metal and its environment and, thereby, prolongs service life of the alloy. The ability to form such a layer depends upon a complex interaction of variables; the most influential being the concentration of Cr present in the alloy. In fact, there is a critical concentration of Cr, below which, a complete, protective Cr_2O_3 scale will not form. Under the severe conditions employed in this investigation, upwards of 18 weight percent Cr is required to form a protective layer in the binary Ni-Cr and Fe-Cr alloys. (SES)

Previous investigations have shown that the presence of small amounts of finely dispersed oxides or nitrides such as ThO_2 , Y_2O_3 , TiO_2 , Si_3N_4 and TiN can significantly effect the oxidation behavior of binary Ni-Cr, Fe-Cr, and Co-Cr alloys. The beneficial effects of these oxide/nitride additions were increased oxidation resistance, an enhanced scale adhesion, and a decreased concentration of Cr necessary to form the protective Cr_2O_3 layer. However, previous investigations have been limited to studying alloys containing Cr concentrations between 14-20 weight percent and dispersed oxide additions of only 1-2 volume percent.

In the present investigation, a broader composition range of dispersion containing alloys was studied in the hope of gaining a better understanding on the effects of oxide dispersions and the mechanisms involved in the oxidation process. To do this, the Cr concentration was varied between 0 to 15 weight percent with dispersed oxide additions up to 40 volume percent. The dispersed oxide/nitride employed in this investigation was Si_3N_4 and SiO_2 because of their relative abundance, high temperature stability although their effect on transition metal alloys is relatively unknown.

The experimental procedure involved processing elemental powders by simple powder metallurgical techniques. This was followed by kinetic studies using an automatic recording semi-micro-balance under the desired conditions of 1 atmosphere O_2 and temperatures of 1273 and 1373 $^{\circ}$ K. The specimens were held isothermally at the test temperature for approximately 50 hours. Surface topographies of oxidized specimens were then examined by Scanning Electron Microscopy. Transverse sections of representative specimens were also prepared and examined both optically and by SEM techniques in order to determine the distribution of elements in the oxide scales. Finally, standard x-ray diffraction techniques were employed to identify the phases present in the scale. To try and better understand the growth characteristics of the scales, series of short term oxidation tests of 5, 10, 15, and 30 minutes were done in O_2 at 1273 $^{\circ}$ K.

The following discussion summarizes the work and results obtained on a number of Fe-Cr-Si $_3$ N $_4$, Ni-Cr-SiO $_2$ and Fe-Cr-SiO $_2$ alloys and, also, discusses the possible mechanisms involved in the oxidation process of these alloys.

Fe-Si $_3$ N $_4$ and Fe-Cr-Si $_3$ N $_4$ Alloys

Si $_3$ N $_4$ was first chosen as fine, dispersed particles due to its low solubility and strengthening effect in the Fe base alloys. Si $_3$ N $_4$ also can serve as the Si source for the growth of a protective SiO $_2$ scale. In this study, Fe-Cr alloys with and without the addition of 10 vol% Si $_3$ N $_4$ particles were made by conventional powder metallurgy method and then oxidized at 1173 and 1273 $^{\circ}$ K in 1 atm of O_2 . The oxidation kinetic results (shown on Fig.1) confirm that the addition of Si $_3$ N $_4$ significantly reduces the

oxidation rates in comparison to that of pure Fe. Similar behavior is observed on the series of Fe-Cr alloys (i.e., Fe-3Cr, Fe-5Cr, Fe-7Cr, Fe-9Cr, and Fe-14Cr). The incorporated Si_3N_4 reduces not only the oxidation rate but also the weight gain during the initial oxidation period even in an alloy containing only 3 wt% of Cr.

The previous investigations of Fe-Cr alloys usually utilized high Cr content (about 14-20 wt%) in order to get continuous protective layer on the surface. In the present study, the results indicate that the critical bulk concentration of Cr necessary for forming a continuous Cr_2O_3 layer is significantly reduced to about 5% in the presence of large amounts of Si_3N_4 dispersions in alloys prior to sintering. This reduction may result from increased nucleation of Cr_2O_3 on the remaining Si_3N_4 or the formed SiO_2 particles. As a matter of fact, the motion of Fe is slowed down in the continuous external Cr_2O_3 scale under which SiO_2 layers may form to provide additional oxidation resistance.

The variation of Cr content in the Fe-Cr alloys containing dispersion of Si_3N_4 greatly effects the oxidation behavior. These results are illustrated in Fig. 2 and 3. From Fig. 3, little difference between the weight gains after two different oxidation times is observed. This indicates that the formation of the protective scale is virtually completed within 20 hours in the Fe-Cr alloys with the presence of SiO_2 from the decomposition of Si_3N_4 particles as well as the unreacted nitride particles.

Upon the completion of kinetic measurements, the oxidized specimen were examined with scanning electron microscope to evaluate the grain size from the surface topographies as well as the stacking sequence and thickness of the different oxide layers from the transverse section views. Fairly fine oxide grains and a smooth oxide surface are observed on the alloys with Si_3N_4 while large oxide grains are formed on the alloys

without Si_3N_4 . Thus, the number of grain boundaries which may increase diffusion of Cr is higher in the alloy systems with Si_3N_4 dispersions.

Inert platinum markers, initially placed on the alloy surface prior to oxidation, were found on the top of the Cr_2O_3 which formed on an Fe-9Cr alloy with Si_3N_4 after 50 hours of oxidation at 1273°K while the Pt markers were in the middle of the oxide scale formed on an Fe-9Cr alloy without Si_3N_4 after 72 hours of oxidation at 1273°K . This difference in marker position shows the change of oxide growth mechanism due to the presence of Si_3N_4 dispersion. The growth mechanism changes from predominantly outward ion motion to anion inward motion.

Phase identification of the oxide scale was done by X-ray diffraction analysis utilizing diffractometer and Debye-Sherrer techniques. The oxide in Fe-Cr alloys with Si_3N_4 consisted of Fe_2O_3 , Cr_2O_3 and SiO_2 . In addition, Fe_2O_3 and SiO_2 were detected in pure Fe with 10 vol% of Si_3N_4 . On the other hand, the oxides in Fe-Cr alloys without Si_3N_4 consisted of Fe_2O_3 , Fe_3O_4 , Cr_2O_3 and some FeCr_2O_4 . The amount of Fe_2O_3 decreased as the Cr content was increased until no Fe_2O_3 was detected in the Fe-9Cr with Si_3N_4 . FeO was not found in these alloys except for the case of pure Fe oxidation. As the Cr content was increased, the ratio of $\text{Fe}_2\text{O}_3/\text{Fe}_3\text{O}_4$ increased and no Fe_3O_4 was detected in the Fe-14Cr alloys.

Fe- SiO_2 and Ni- SiO_2 Alloys

Additions of SiO_2 (up to 20 volume percent) to pure Fe reduced the weight gained by the Fe based alloys as can be seen in Figure 4 and, also, increased their oxidation resistance as can be seen in the decrease in parabolic rate constant as a function of SiO_2

in Figure 5. However, the effect was a modest one and large weight gains occurred regardless of the amount of SiO_2 present. Scale examination revealed no significant changes in scale appearance or composition when compared to those of pure Fe, but SiO_2 particles were found at the alloy/scale interface and in the scale near the interface. Therefore, the increased oxidation resistance (i.e. decreased K_p values) was the result of the SiO_2 particles effectively blocking the transport of ionic species at the alloy/scale interface as well as in the oxide scale itself.

Additions of SiO_2 (up to 20 volume percent) to pure Ni increased slightly the weight gained by these alloys. Examination of the oxide scale revealed no significant changes in either scale appearance or composition as compared to that which formed on the pure Ni. Therefore, the slight decrease in oxidation resistance was thought to be caused by the SiO_2 particles increasing the cation vacancy concentration in the p-type NiO scale. An increase in the vacancy concentration would have effectively accelerated the diffusion of ionic species through the scale and ultimately result in a decrease in oxidation resistance for the Ni alloys containing SiO_2 . In general, the addition of SiO_2 to either pure Fe or Ni had a relatively small effect on the overall oxidation behavior of the alloys.

Ni-6Cr- SiO_2 and Fe-6Cr- SiO_2 Alloys

The presence of SiO_2 dispersions in Ni-6Cr alloys significantly effected their oxidation behavior as shown in Figure 6. During the early stages of oxidation, the oxidation kinetics of the Ni-6Cr alloys containing 5 and 10 volume percent SiO_2 were similar to that of the binary Fe-6Cr alloy. However, after a relatively short period of time, the oxidation rates were markedly reduced. These sudden reductions in the oxidation rates were apparently due to the completion of a protective oxide scale

underneath the initially formed NiO. SEM and x-ray analysis of these scales revealed a thin Cr_2O_3 layer adjacent to the alloy/scale interface which caused the dramatic reduction in oxidation rates. The time required to develop a complete, protective Cr_2O_3 layer was reduced as the volume percent of SiO_2 dispersion in the alloy increased. A schematic of the overall oxidation process of Ni-6Cr- SiO_2 alloys with (a) low volume percents and (b) high volume percents of SiO_2 is shown in Figure 7. Alloys containing low volume percents of SiO_2 formed a protective Cr_2O_3 layer underneath the initially formed NiO scale. As the SiO_2 was increased, a Cr_2O_3 layer developed more readily further reducing the amount of Ni containing oxides which formed.

Additions of SiO_2 to Fe-6Cr alloys had little effect on their oxidation behavior as shown in Figure 8. The scales that formed were thick and consisted primarily of Fe-Cr spinel and Fe_2O_3 . Only a small amount of Cr_2O_3 was detected; therefore, it can be concluded that no protective layer developed at any stage in the oxidation process of the alloys.

Ni-9Cr- SiO_2 , Ni-12Cr- SiO_2 , and Ni-15Cr- SiO_2 Alloys

The oxidation behavior of alloys containing 9 to 15 weight percent Cr displayed a dramatic decrease in oxidation rate upon the addition of up to 40 volume percent SiO_2 . Weight gains ranged from approximately 4 mg/cm^2 for a Ni-9Cr-5% SiO_2 alloy to a low of 0.6 mg/cm^2 for a Ni-15Cr-40% SiO_2 alloy. The small weight gains observed were expected since an increase in Cr content would have resulted in the development of a protective Cr_2O_3 layer in a shorter period of time. Consequently, the amount of Ni containing oxides that formed decreased, causing a reduction in the overall weight gained by the alloys. Also, increasing additions of SiO_2 , from 5 to 40 volume percent, had a

diminishing effect on the overall weight gained by the alloys the higher the Cr content. In other words, the difference between the weight gained by an alloy containing only 5 volume percent SiO_2 and that of an alloy containing 40 volume percent SiO_2 decreased the higher the Cr content in the alloy. This difference was upwards of 3 mg/cm^2 in the Fe-9Cr alloys containing 5 and 40 volume percent SiO_2 , and less than 1 mg/cm^2 in the Fe-15Cr alloys containing 5 and 40 volume percent SiO_2 .

Fe-9Cr-SiO₂ and Fe-12Cr-SiO₂ Alloys

Additions of up to 20 volume percent of SiO_2 to Fe-9Cr alloys dramatically reduced the overall weight gained by the alloys as can be seen by comparing Figures 9 and 10. The parabolic rate constants shown in Figure 11 also decreased dramatically upon the addition of SiO_2 which indicated a significant change in the scale behavior upon the addition of SiO_2 . SEM and X-ray analysis of the scales formed on the SiO_2 containing alloys revealed the presence of a thin Cr_2O_3 layer adjacent to the alloy/scale interface. The overall oxidation process of the Fe-9Cr-SiO₂ alloys is shown in Figure 12 and is similar to that proposed for the Ni-Cr alloys containing low volume percents SiO_2 . During the early stages of oxidation, the alloy surface was covered by Fe rich oxides. Consequently, the Cr_2O_3 layer developed underneath the initially formed Fe rich oxide layer which dramatically increased the oxidation resistance of the Fe-9Cr alloys containing SiO_2 .

The oxidation behavior of Fe-12Cr alloys with SiO_2 additions (up to 20 volume percent) are shown in Figure 13. These results were inconsistent and unexpected due to the relatively large weight gains found for the Fe-12Cr alloys containing 5 and 10 volume percent of SiO_2 . The large weight gains were determined to be the result of an

absence in the development of a complete, protective Cr_2O_3 layer. One possible explanation for the absence of this layer was that during the early stages of oxidation the thin Cr-rich film that may have been formed transformed from a protective to a non-protective type of film. Consequently, the increase in diffusion of Fe ions through the non-protective scale could have resulted in the relatively large weight gains observed in the Fe-12Cr alloys containing 5 and 10 volume percent SiO_2 .

The significant improvement in oxidation resistance in both the Ni-Cr and Fe-Cr alloys containing SiO_2 was the result of the development of a protective Cr_2O_3 layer. The level of Cr required to develop such a layer was significantly lower than that which would be required to form a protective layer in the binary Ni-Cr and Fe-Cr alloys. Therefore, it was concluded that the SiO_2 dispersions had a significant role in the overall oxidation behavior of these alloys.

Enhancement of Cr_2O_3 formation

The role that Si_3N_4 or SiO_2 dispersions played in the overall oxidation process of both the Ni-Cr and Fe-Cr alloys was difficult to determine. However, it would appear that the Si_3N_4 or SiO_2 dispersions enhanced the transport of Cr through an increase in short circuit diffusion paths as well as providing additional low energy nucleation sites for the first formed oxides, in particular Cr_2O_3 . These conclusions on how dispersion phase enhanced the formation of a protective Cr_2O_3 layer are briefly discussed in the following paragraphs.

The addition of Si_3N_4 or SiO_2 dispersions, resulted in a significant reduction in the grain size of both the Ni-Cr and Fe-Cr alloys. Since grain boundaries have been known

to be rapid diffusion paths for the transport of Cr, any increase in boundary area would have effectively enhanced the transport of Cr to the surface and increased the amount of Cr available to develop a protective Cr_2O_3 layer. Once at the surface, interfacial boundaries (i.e. the boundaries created between the alloy/ SiO_2 particles) acted as rapid diffusion paths for the lateral transport of Cr. Thus, the accelerated transport of Cr along such boundaries could ultimately result in the development of a continuous protective Cr_2O_3 layer. However, another possible mechanism exists that could have aided in the formation of a protective layer.

The presence of SiO_2 particles at the surface also acted as physical discontinuities and, as such, were low energy sites for oxide nucleation (i.e. heterogeneous versus homogeneous nucleation). This could have reduced the distance between Cr_2O_3 nuclei which would have limited to an extent the lateral growth necessary for the impingement of Cr_2O_3 grains and the development of a Cr_2O_3 layer. The SiO_2 particles were, therefore, preferential sites for oxide nucleation which could have aided in the development of a protective Cr_2O_3 layer in both the Ni-Cr- SiO_2 and Fe-Cr- SiO_2 alloys.

In general, the Si_3N_4 or SiO_2 dispersions appear to have enhanced mechanisms already inherent to the oxidation process of the Ni-Cr and Fe-Cr alloys. However, the SiO_2 dispersions had a greater influence on the oxidation behavior of the Ni-Cr alloys suggesting its effects were not independent of the base metal.

SiO_2 Growth Mechanism Study

According to previous studies, it is generally agreed that the growth of SiO_2 scale is mostly due to the inward interstitial diffusion of oxydant species which contain both charged oxygen ions and noncharged oxygen molecules or atoms. The possible influence

of electronic species (i.e., electrons and electron holes) on the SiO_2 growth at high temperature was also studied in this project.

Basically, the experiment consisted of placing an inert electronic oxide conductor which acts as electronic short circuit path on the surface of pure silicon and then oxidizing them in dry oxygen atmosphere. Since Si is too brittle to drill a hole for inserting a inert conductor, fine Cr_2O_3 powders were pressed on the Si surface to serve as electronic conductor, as shown on Fig. 14. After oxidizing at 1200°C for 90 hours, the cross section area of the sample was examined by scanning electron microscopy (SEM) to determine whether the growth rate of SiO_2 is accelerated in the regions close to the conductor or not. Because of the poor conductivity of Si and SiO_2 , a thin film of Au is coated on the samples to show better SEM images. It is still very difficult to have very clear and highly magnified SEM images. The result is shown on Fig. 15.

Only a very small difference of the growth rate was observed on the edges of Cr_2O_3 powder. The oxide layer is thicker in the region right next to the electronic conductors. We might find that the electronic species may act as a kind of transport defect which will promote the growth of SiO_2 . Since the exact thickness of the oxide layer is difficult to recognize, it is hard to get kinetic data through optical observation of these very thin oxide layer whose thickness is about 2-3 μm .

REFERENCE

1. H. H. Davis, H. C. Graham, and I. A. Kvernes, *Oxid. Met.*, **3**, 431, (1971).
2. G. C. Wood, *Corrosion Science*, **2**, 173, (1962).
3. C. Wagner, *J. Electrochem. Soc.*, **103**, 627, (1956).
4. C. S. Giggins, and F. S. Pettit, *Met. Trans.*, **2**, 1071, (1971).
5. A. Atkinson, *Oxid. Met.*, **24**, 177, (1985).
6. I. G. Wright, and B. A. Wilcox, *Met. Trans.*, **5**, 957, (1974).
7. H. Nagai, Y. Takebayashi, and H. Mitani, *Met. Trans.*, **12a**, 435, (1981).
8. J. Stringer, B. A. Wilcox, *Met. Trans.*, **5**, 957, (1974).
9. S. W. Park, Ph.D. Thesis, The Pennsylvania State University, University Park, PA (1987).
10. P. J. Jorgenson, *J. Chem. Phys.*, **37**, 874, (1962).
11. E. A. Irene, *J. Electrochem. Soc.*, **125**, 1708, (1978).
12. S.-W. Park and G. Simkovich, in "Alternate Alloying for Environmental Resistance", ed. by G. R. Smolik and S. K. Banerji, AIME, Wallendare, PA, pp. 233-247 (1987).

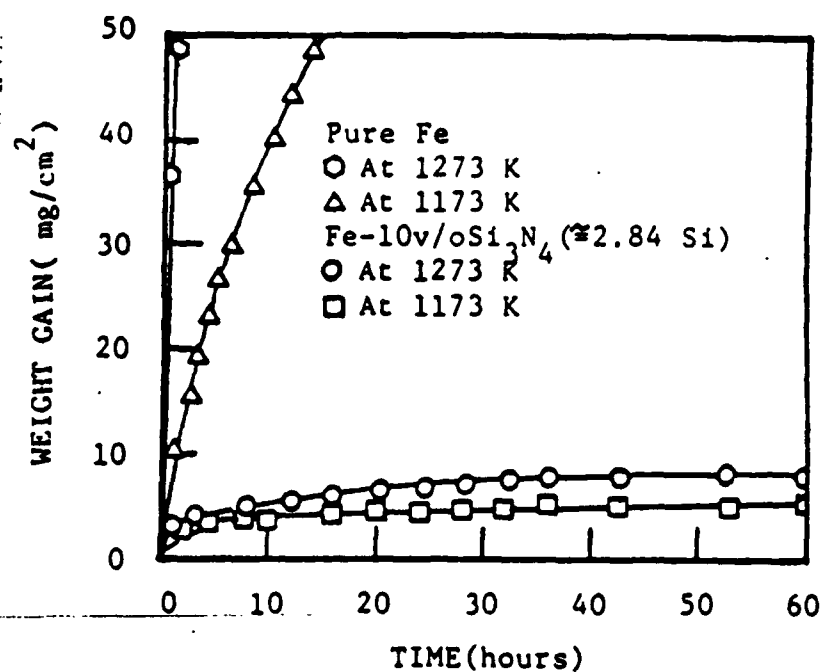


Fig. 1 Isothermal oxidation curves for pure Fe with and without an initial addition of 10% Si₃N₄ (≈ 2.84 Si) at 1173 and 1273 K.

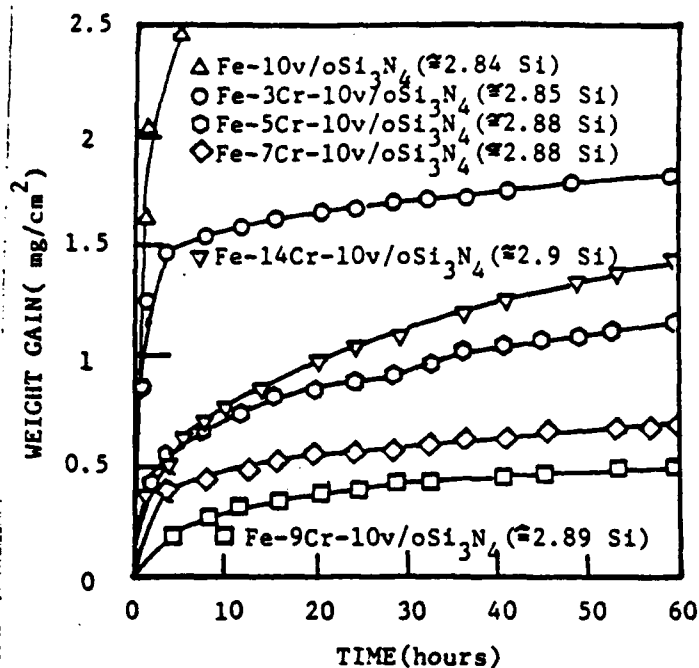


Fig. 2 Isothermal oxidation curves for Fe-Cr alloys with an initial addition of 10 v/o Si_3N_4 as a function of Cr content in 1 atm O_2 at 1273 K.

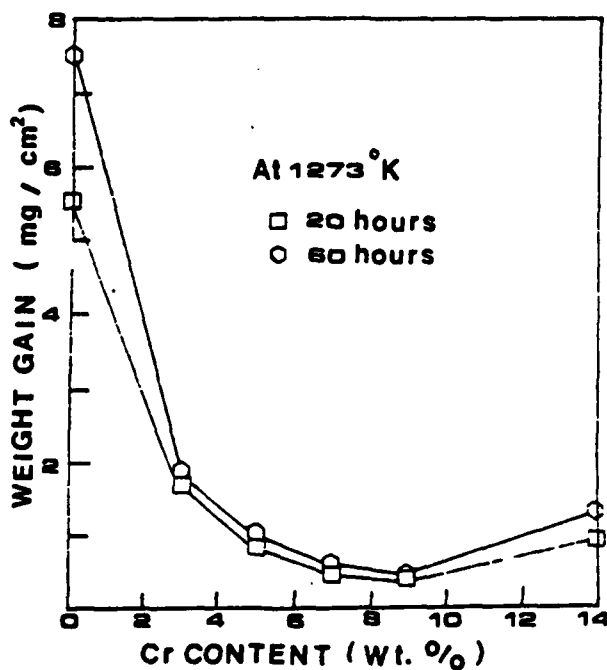


Fig. 3 Weight gain in Fe-Cr alloys with an initial addition of 10 v/o Si_3N_4 (see Table 2); one for initial 20 hours and the other for 60 hours in 1 atm O_2 at 1273 K.

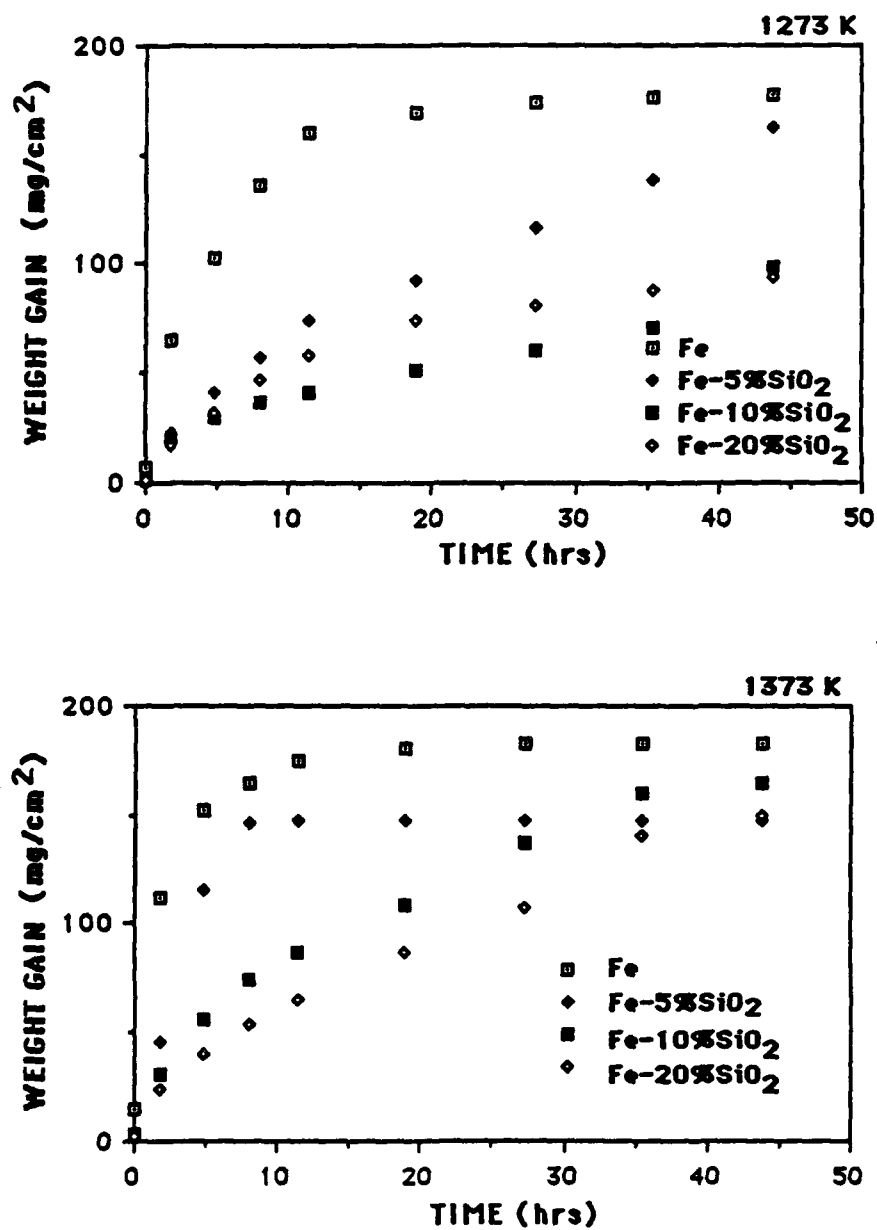


Fig. 4 Weight gain per unit area in O₂ for Fe-SiO₂ alloys at 1273 and 1373 K

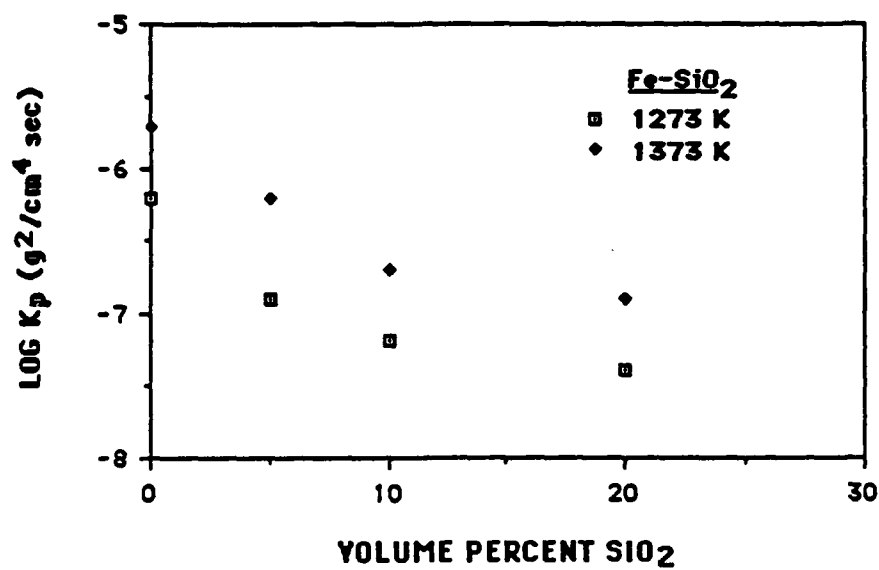


Fig. 5 The relationship between parabolic rate constant (K_p) and volume percent SiO_2 in Fe-SiO_2 alloys

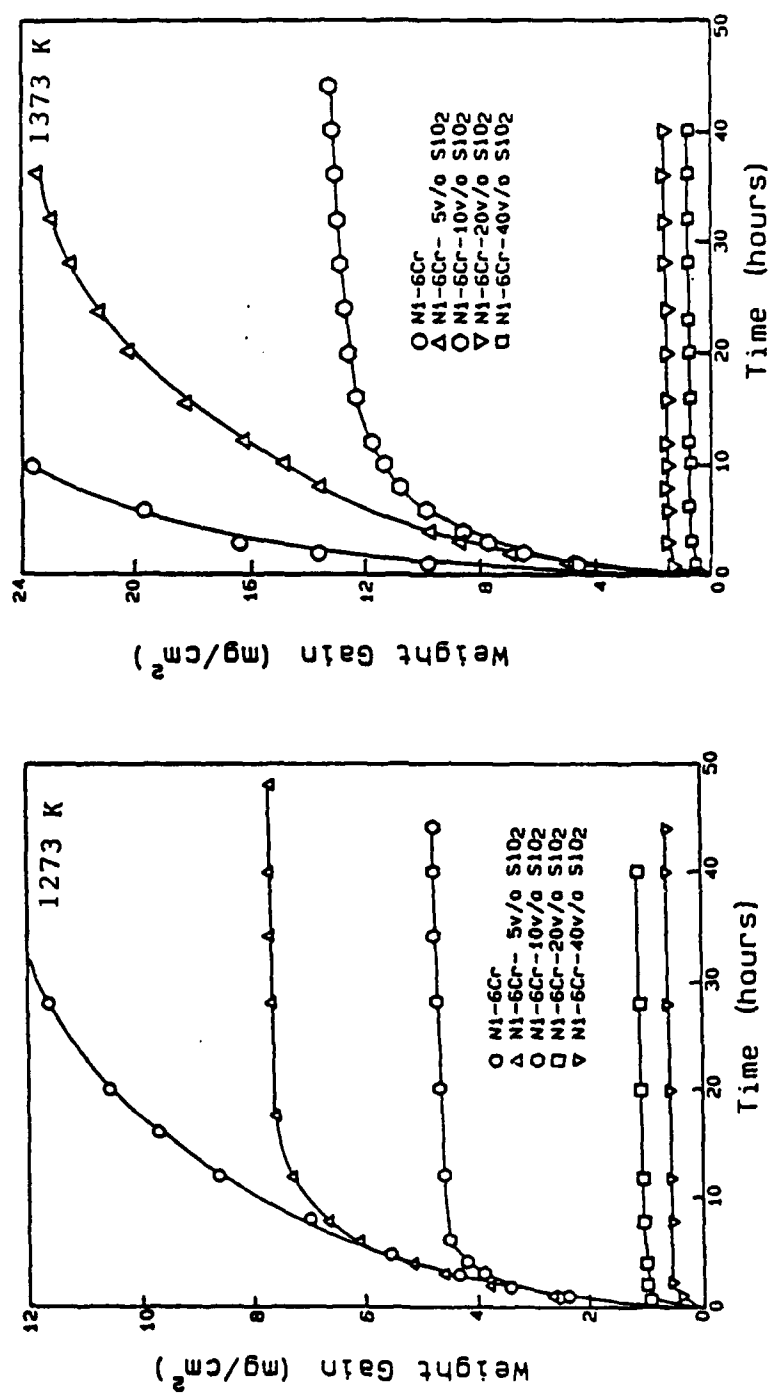


Fig. 6 Weight gain per unit area in O₂ for Ni-6Cr-SiO₂ alloys at 1273 and 1373 K

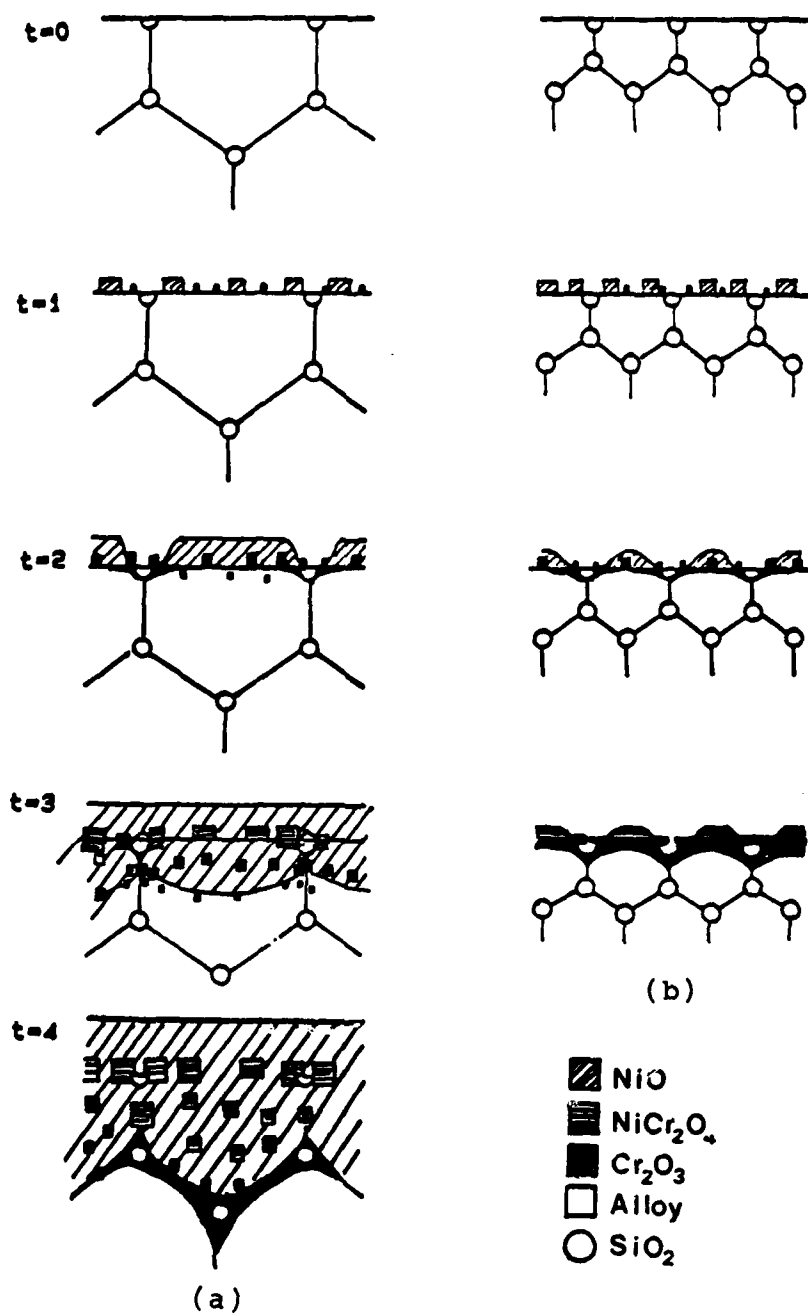


Fig.7 : Schematic representation of oxide formation on Ni-6Cr- SiO_2 alloys at (a) low volume percents and (b) high volume percents of SiO_2

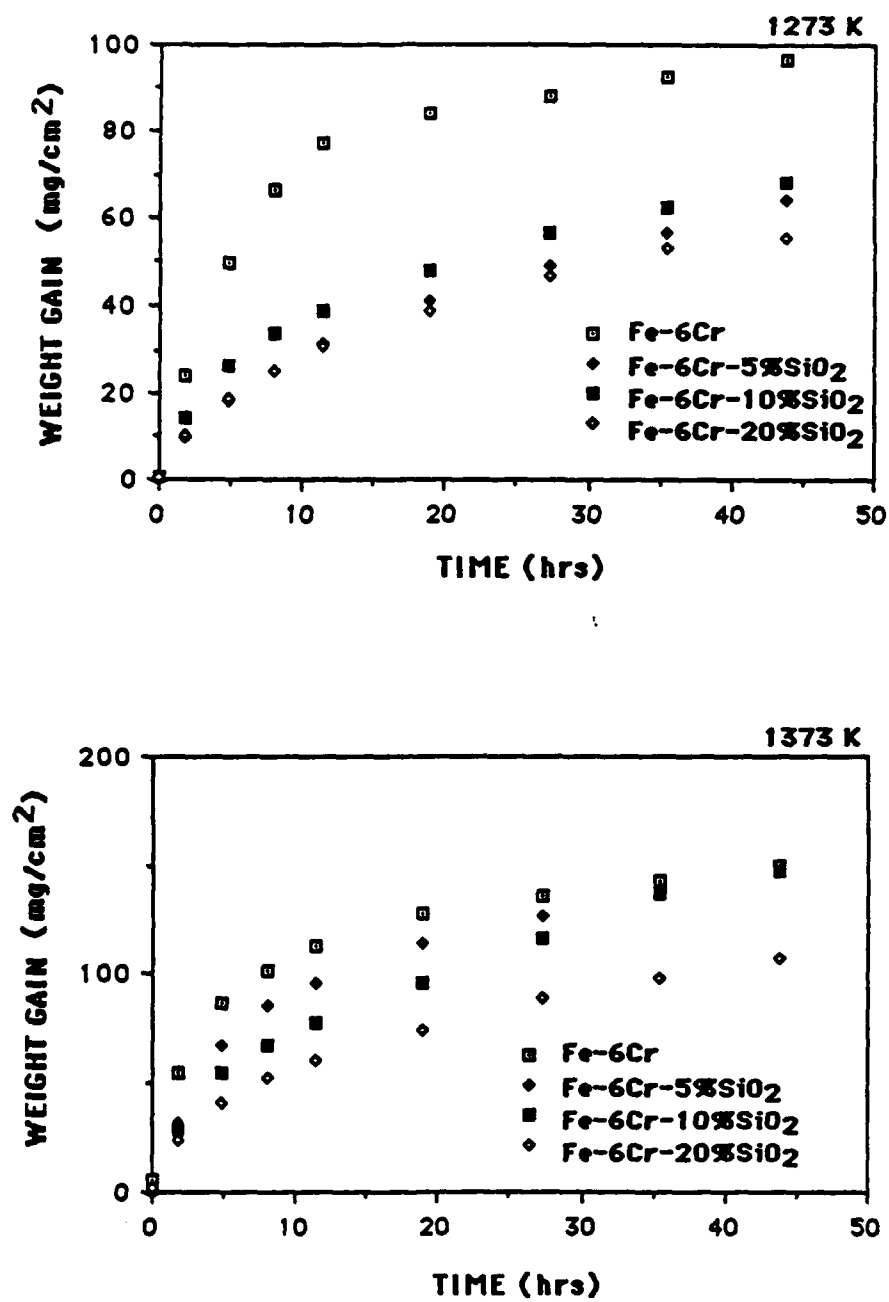


Fig. 8 Weight gain per unit area in O₂ for Fe-6Cr-SiO₂ alloys at 1273 and 1373 K

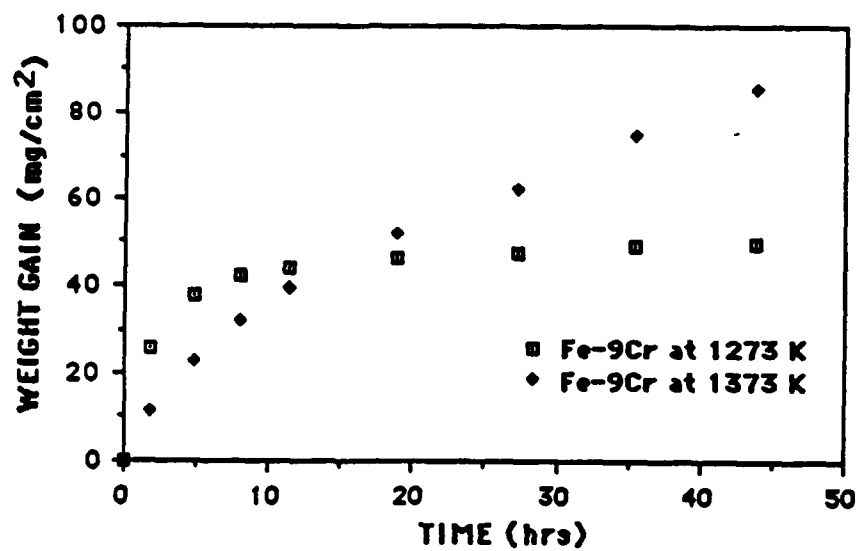


Fig. 9 : Weight gain per unit area in O_2 for binary Fe-9Cr alloys at 1273 and 1373 K

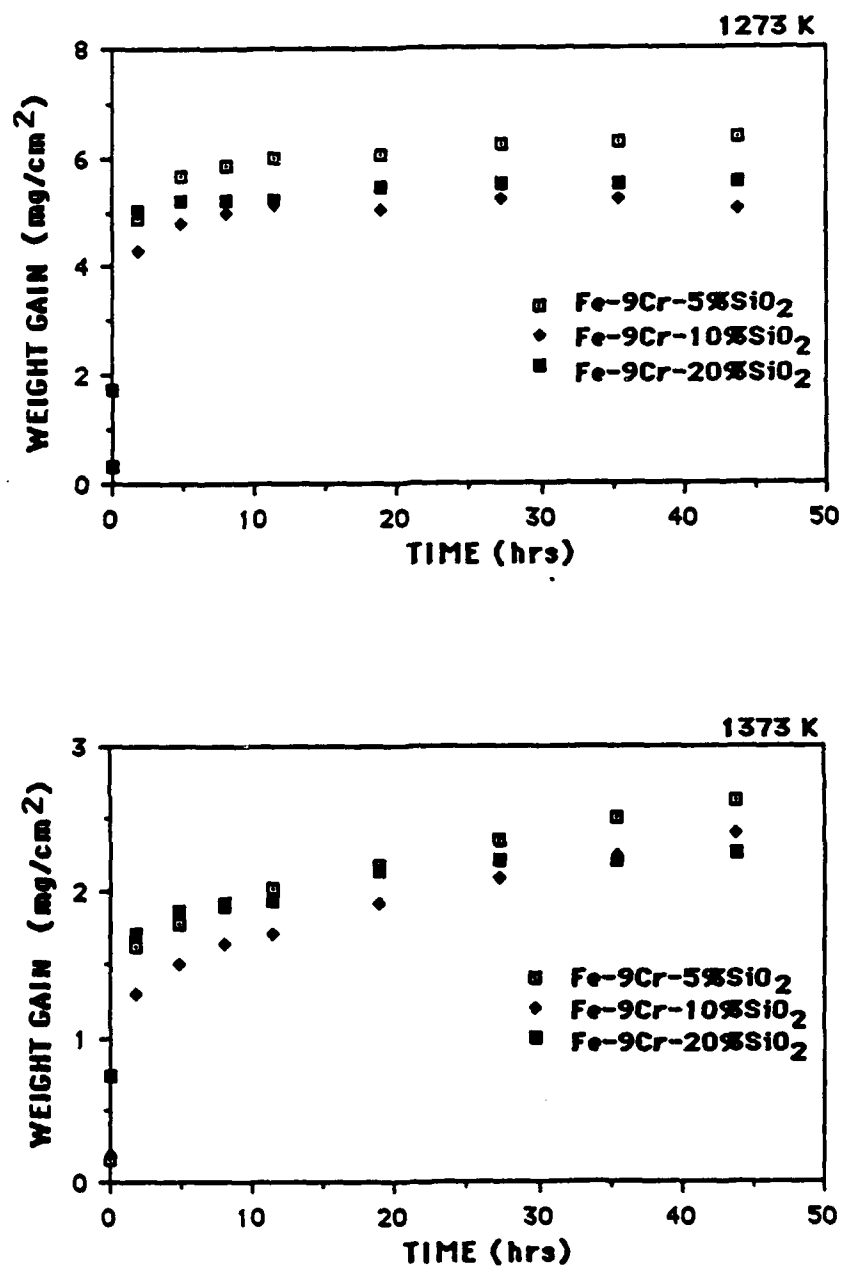


Fig. 10 : Weight gain per unit area in O₂ for Fe-9Cr-SiO₂ alloys at 1273 and 1373 K

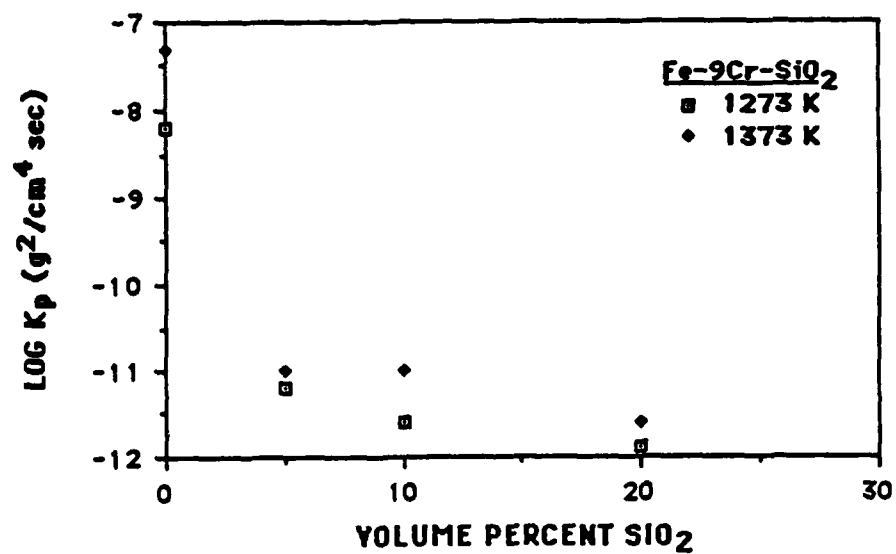


Fig. 11 : The relationship between parabolic rate constant (K_p) and volume percent SiO_2 in Fe-9Cr- SiO_2 alloys

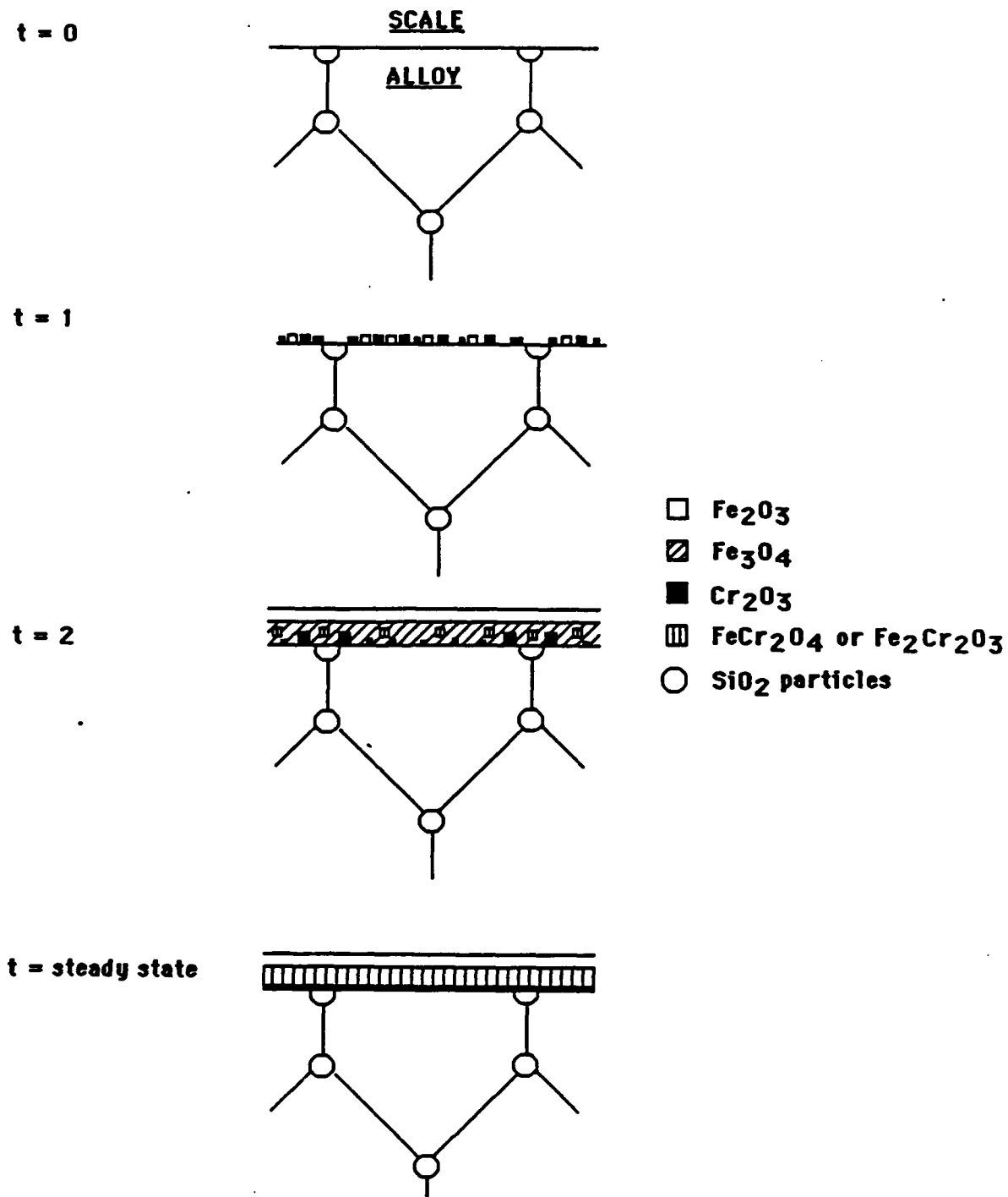


Fig. 12 Schematic representation of oxide formation on Fe-9Cr-SiO₂ alloys

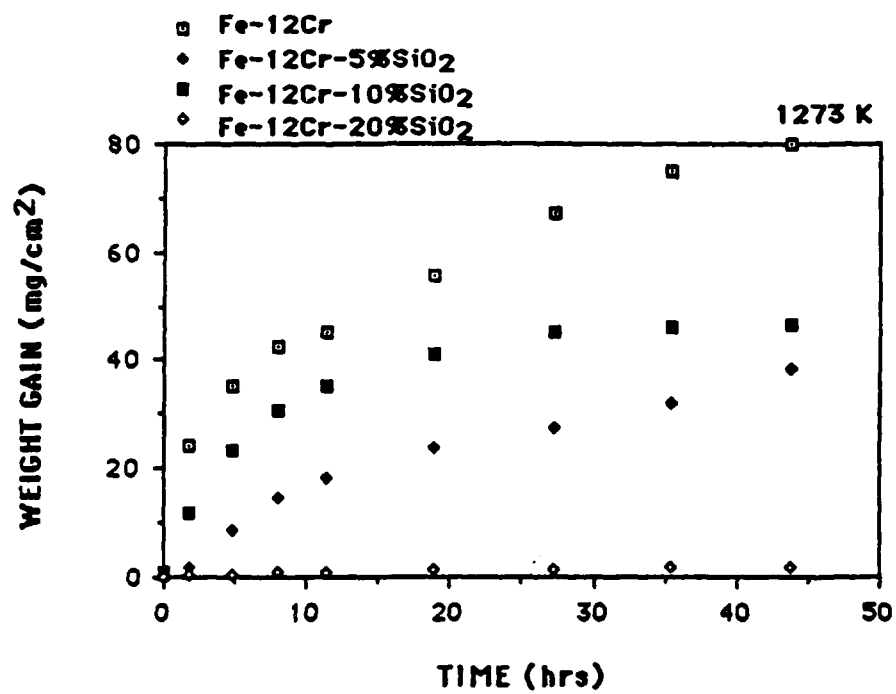


Fig. 13 : Weight gain per unit area in O₂ for Fe-12Cr-SiO₂ alloys at 1273 K

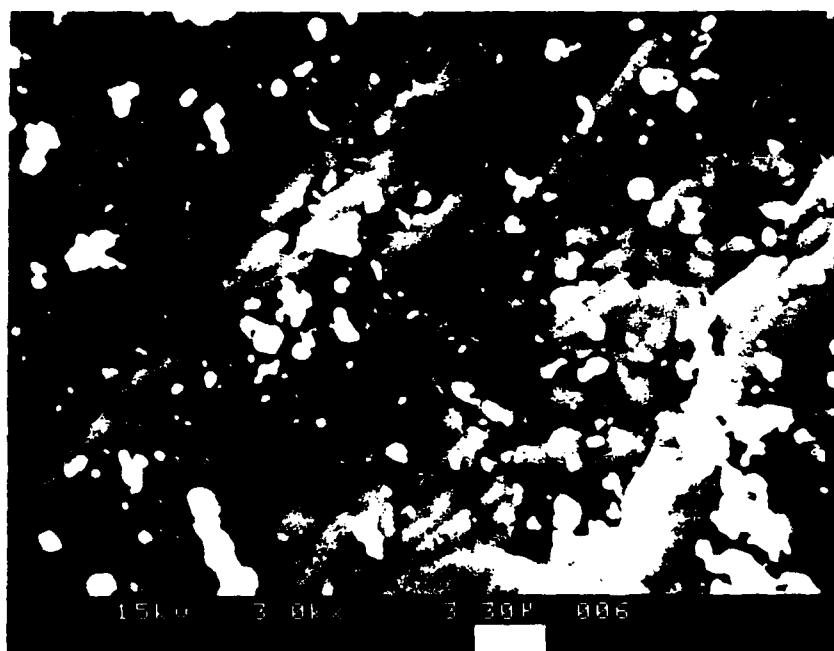
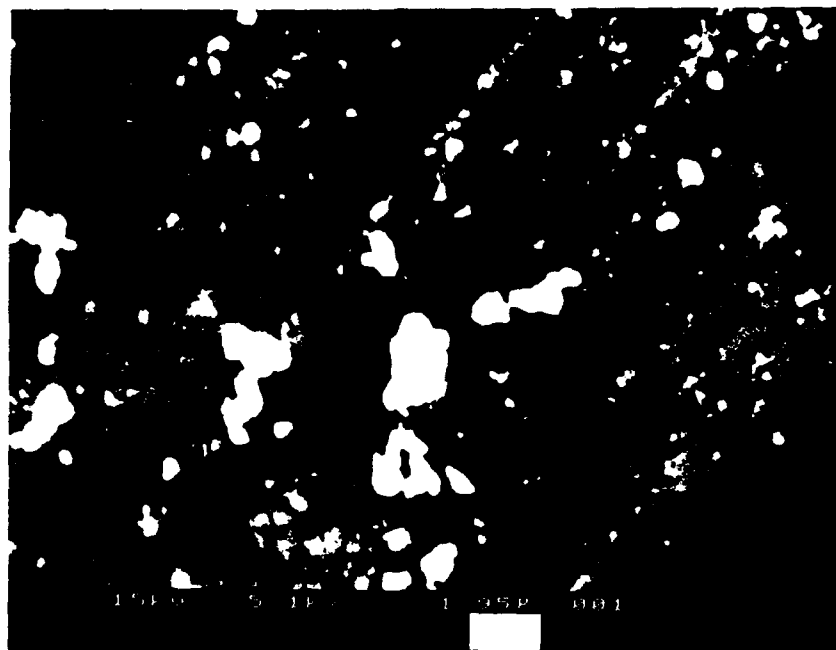


Fig. 14 Surface morphology of the Si sample, white particles are Cr_2O_3 powders

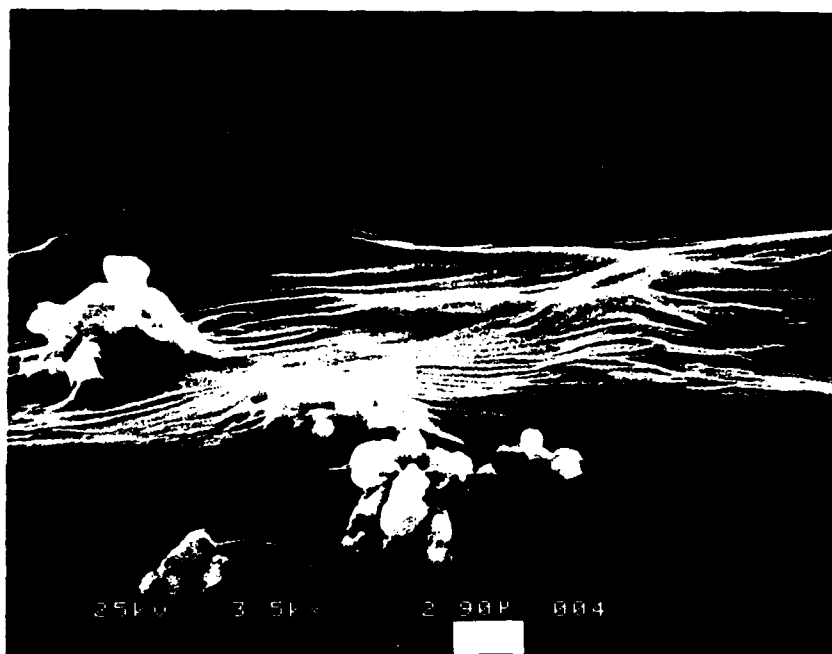


Fig. 15 Cross section view of the oxide layer

